

“Synthesis and Order-Disorder Transition in Novel Metal Formate Framework of $[(\text{CH}_3)_2\text{NH}_2]\text{Na}_{0.5}\text{Fe}_{0.5}(\text{HCOO})_3$ ”, by Mirosław Mączka et al.

Table S1. Data collection, cell, and refinement parameters for the single crystal X-ray diffraction studies carried out at 293 and 110 K.

formula	C10H22FeN2NaO12	C10H22FeN2NaO12
Fw	441.14	441.14
T, K	293(2) K	110(2) K
wavelength	0.71073 Å	0.71073 Å
crystal system	trigonal	triclinic
space group	R-3	P-1
a, Å	8.3570(12)	8.2617(17)
b, Å	8.3570(12)	9.0797(18)
c, Å	23.136(5)	12.293(3)
α , °	90	95.37(3)
β , °	90	90.43(3)
γ , °	120	89.91(3)
V, Å ³	1399.3(4)	918.1(3)
Z	3	2
F(000)	687	458
D _c , g/cm ³	1.570	1.596
crystal size, mm ³	0.38x0.36x0.24	0.38x0.36x0.24
$\Theta_{\min}, \Theta_{\max}$, °	4.51, 29.58	2.96, 26.73
index ranges	-10 ≤ h ≤ 11	-10 ≤ h ≤ 10

	-11 ≤ k ≤ 11,	-11 ≤ k ≤ 10
	-31 ≤ l ≤ 31	-15 ≤ l ≤ 15
reflections collected	5672	8492
unique reflns., R _{int}	844, 0.0195	3754, 0.0393
Completeness to Θ = 26.73	95.4 %	95.9 %
Data / restraints / parameters	844 / 4 / 67	3754 / 0 / 236
Goodness of fit on F ²	1.359	1.363
Final R indices [I>2σ(I)]	R ₁ = 0.0236 wR ₂ = 0.0512	R ₁ = 0.0974 wR ₂ = 0.2159
R indices (all data)	R ₁ = 0.0268 wR ₂ = 0.0517	R ₁ = 0.1141 wR ₂ = 0.2217
largest diff. peak and hole, e Å ³	0.255 and -0.199	2.807 and -1.242

Table S2. Selected bond lengths (\AA) for DMNaFe.

	293 K	110 K	
Na environment			
Na1-O2 \times 6	2.4143(5)	Na1-O7	2.487(3)
		Na1-O8	2.521(3)
		Na1-O9	2.346(3)
		Na1-O10	2.297(3)
		Na1-O11	2.406(3)
		Na1-O12	2.420(3)
Fe environment			
Fe1-O1 \times 6	2.0121(4)	Fe1-O1	2.115(2)
		Fe1-O2	1.987(2)
		Fe1-O3	2.006(2)
		Fe1-O4	1.948(2)
		Fe1-O5	2.141(2)
		Fe1-O6	1.970(2)
Formate			
C0-O1	1.2672(5)	C1-O2	1.303(4)
C2-O2	1.2171(5)	C1-O12	1.192(4)
		C2-O5	1.244(4)
		C2-O9	1.294(4)
		C3-O4	1.336(4)
		C3-O7	1.193(4)
		C4-O1	1.263(4)
		C4-O10	1.280(4)
		C5-O6	1.318(4)

C5-O8	1.214(4)		
C6-O3	1.306(4)		
C6-O11	1.233(4)		
DMA ⁺			
N1-C1	1.4279(13)	N1-C7	1.414(5)
N1-C2	1.3266(14)	N1-C8	1.289(6)
		N2-C9	1.359(6)
		N2-C10	1.353(5)

Table S3. The geometries of the N-H \cdots O bonds between the DMA $^+$ cations and the anionic framework at 110 K (distances, Å; angles, °).

D-H \cdots A	d(D-H)	d(H \cdots A)	d(D \cdots A)	\angle (DHA)
N(1)-H(1A)...O(2)	0.85	2.46	3.170(4)	141.9
N(1)-H(1A)...O(12)	0.85	2.21	2.977(5)	150.0
N(1)-H(1B)...O(6)#5	0.85	2.89	3.494(4)	130.1
N(1)-H(1B)...O(8)#5	0.85	2.26	3.104(5)	171.5
N(2)-H(2A)...O(5)#12	0.85	2.74	3.412(5)	136.7
N(2)-H(2A)...O(9)#12	0.85	2.18	2.998(5)	161.7
N(2)-H(2B)...O(3)	0.85	2.92	3.409(5)	118.5
N(2)-H(2B)...O(11)	0.85	2.07	2.896(5)	164.8

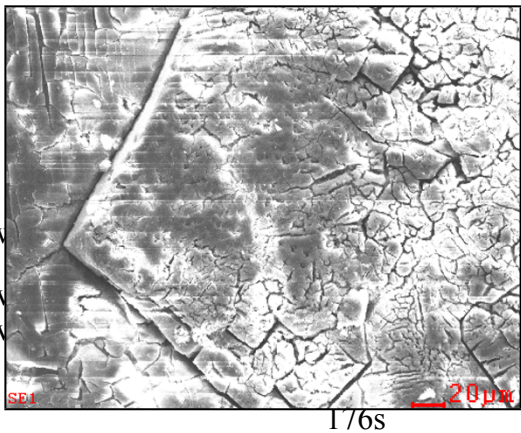
Symmetry transformations used to generate equivalent atoms:

#5 x-1,y,z #12 -x+1,-y,-z+1

Table S4. IR and Raman frequencies (in cm^{-1}) of DMNaFe and suggested assignments.^a

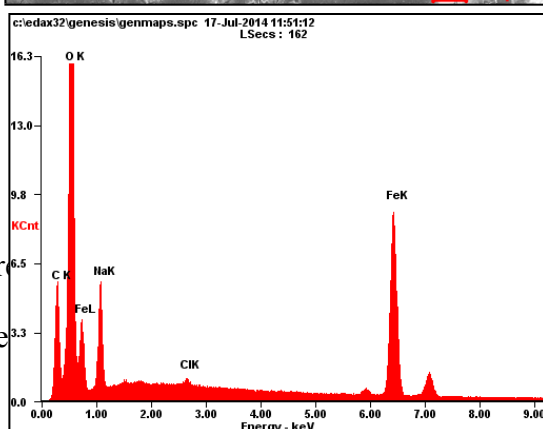
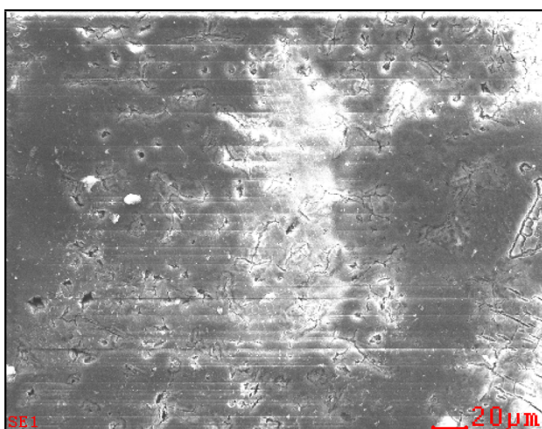
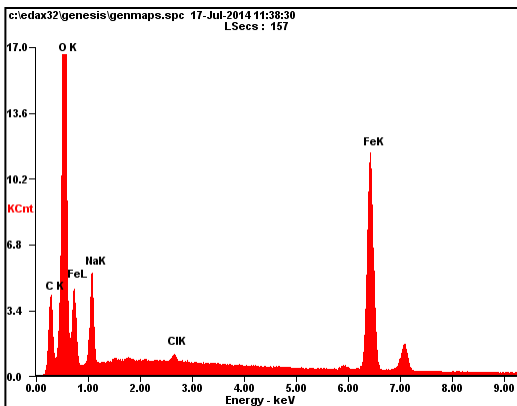
Raman		IR		assignment
295 K	80 K	295 K	5 K	
		3120s	3125m, 3118m	$\nu(\text{NH}_2)$
		3065sh	3068m	$\nu(\text{NH}_2)$
3046sh	3046sh		3037w	$\nu_{\text{as}}(\text{CH}_3)$
3038m	3035m	3032w	3027w	$\nu_{\text{as}}(\text{CH}_3)$
		3006sh	3003m	$\nu(\text{NH}_2)$
2973s	2971s	2975w	2974w	$\nu_s(\text{CH}_3)$
2037vw	2942w	2937w	2945m	$\nu_s(\text{CH}_3)$
2909vw	2910vw			$\nu_4(\text{HCOO}^-) + \nu_5(\text{HCOO}^-)$
2865m	2876m, 2865m	2862s	2879sh, 2865s 2856s, 2844w	$\nu_1(\text{HCOO}^-)$
2850sh	2845w			
	2817w	2792s	2828m, 2811w 2804m, 2781s	$\nu(\text{NH}_2)$
2739w	2743w	2740vw	2742w	$2\nu_5(\text{HCOO}^-)$
		2495w	2536vw 2525w 2510vw	$\rho(\text{NH}_2) + \delta(\text{NH}_2)$
		2463w	2470w, 2460w 2454w	combinations of $\rho(\text{CH}_3)$, $\delta(\text{CH}_3)$ and $\nu_{\text{as}}(\text{CNC})$
1679m	1677m	1678sh	1679w	$\nu_4(\text{HCOO}^-)$
		1648sh, 1632vs	1653sh, 1634vs	$\nu_4(\text{HCOO}^-)$ and $\delta(\text{NH}_2)$
1585vw		1595s	1612s, 1589s 1575m, 1559w	$\nu_4(\text{HCOO}^-)$
			1488sh, 1483w	$\omega(\text{NH}_2)$
1480vw	1488vw	1470w	1474w	$\delta_{\text{as}}(\text{CH}_3)$

1462w	1461m	1459w	1458w	$\delta_{as}(CH_3)$
		1441w	1441w	$\delta_{as}(CH_3)$
1436vw	1436vww		1433w, 1429w	$\tau(NH_2)$
		1418vw	1414vw	$\delta_s(CH_3)$
1381s	1388m, 1385w	1380m	1387w, 1383m	$\nu_5(HCOO^-)$
	1379s		1377m	
1342m	1341m		1340w	$\nu_5(HCOO^-)$
1318m	1318m, 1310m	1318s	1329w, 1320sh	$\nu_2(HCOO^-)$
			1314s	
1283m	1287m, 1275m	1289s	1292s, 1277m	$\nu_2(HCOO^-)$
			1269m	
1236vw		1255sh	1257sh	$\rho(CH_3)$
1096w		1095vw	1099vw	$\rho(CH_3)$
	1079w		1092vw	$\rho(CH_3)$
1067sh,	1068w		1068vw	$\nu_6(HCOO^-)$
1061w				
1048vw	1052vw		1051vw	$\rho(CH_3)$
1024w	1026w	1024m	1026m	$\nu_{as}(CNC)$
		884w,b	913w, 907w	$\rho(NH_2)$
894m	896m	892w	895w	$\nu_s(CNC)$
796sh	802w	795s	802s, 798s	$\nu_3(HCOO^-)$
788m	791m	792sh	794w, 788w	$\nu_3(HCOO^-)$
406w	400w			$\delta(CNC)$
		350s,b	360s, 335sh	$T'(Na^+)$ and $T'(Fe^{3+})$
337m	356w, 343m 333m			$T'(Na^+)$, $T'(Fe^{3+})$ and $\tau(CH_3)$
		288sh	306w, 298w	$T'(Na^+)$ and $T'(Fe^{3+})$



261v	281w		
232v	263w, 254w	T'(Fe ³⁺) and T'(HCOO ⁻)	
217v	237w, 227w	T'(Fe ³⁺) and T'(HCOO ⁻)	
	216m		
161m	190m	T'(HCOO ⁻)	
	166w	L(HCOO ⁻)	
	138w, 126vw	L(DMA)	
110s	118vw	L(HCOO ⁻)	
	93w	T'(DMA)	
	74w	T'(DMA)	
47w	60w, 52w	L(HCOO ⁻)	
	33w	L(HCOO ⁻)	

^aKey: s, strong; m, medium; w, weak; vw, very weak; sh, shoulder; b, broad



Figure

Table

<i>Element</i>	<i>Wt%</i>	<i>At%</i>
<i>NaK</i>	26.50	46.69
<i>FeK</i>	73.50	53.31
<i>Matrix</i>	Correction	ZAF

<i>Element</i>	<i>Wt%</i>	<i>At%</i>
<i>NaK</i>	31.56	52.83
<i>FeK</i>	68.44	47.17
<i>Matrix</i>	Correction	ZAF

DMNaFe measured from two different crystals.

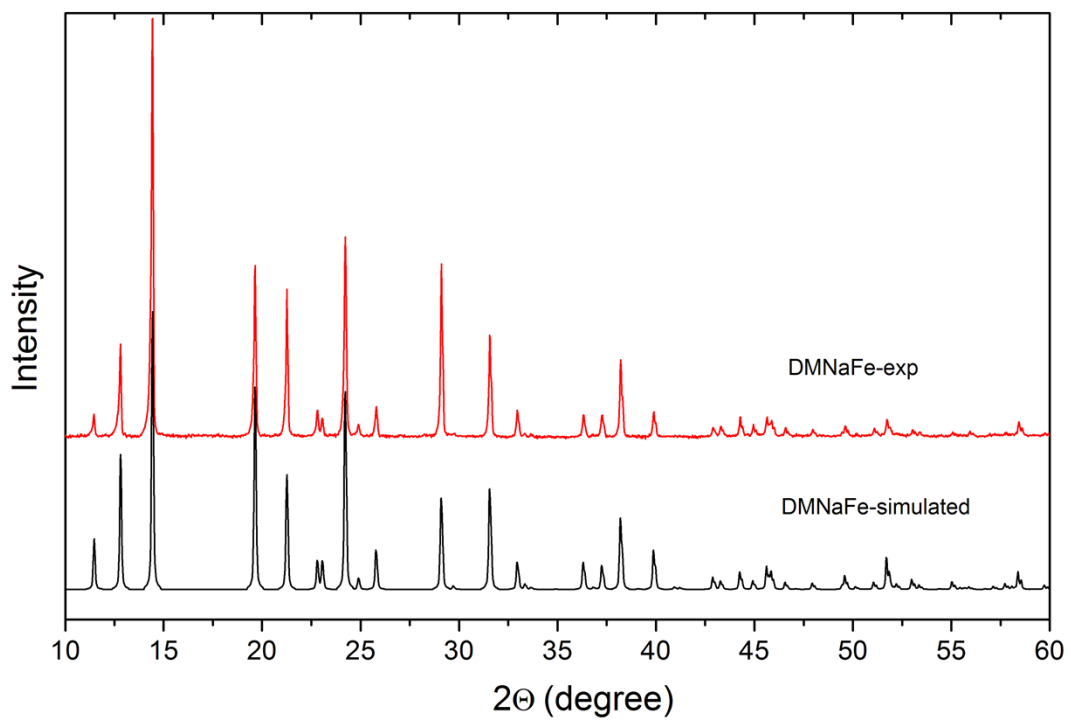


Figure S2. Powder XRD patterns for the as-prepared bulk sample of DMNaFe with the calculated one based on the single crystal structures at 293 K.

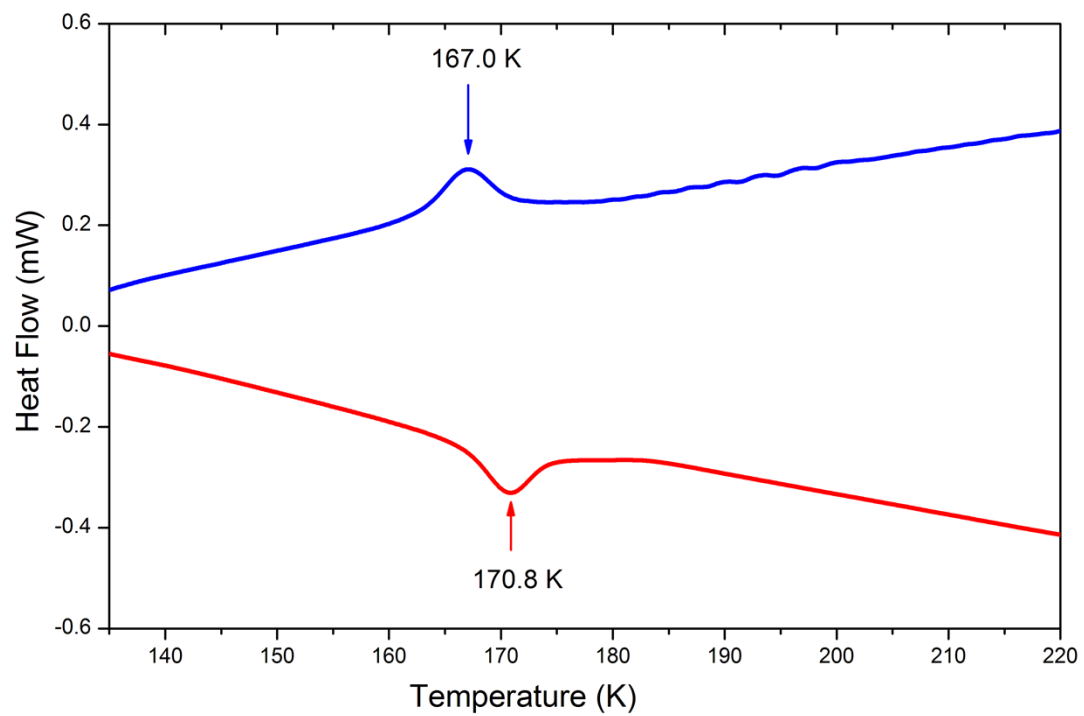


Figure S3. DSC traces for DMNaFe in heating (red) and cooling mode (blue).

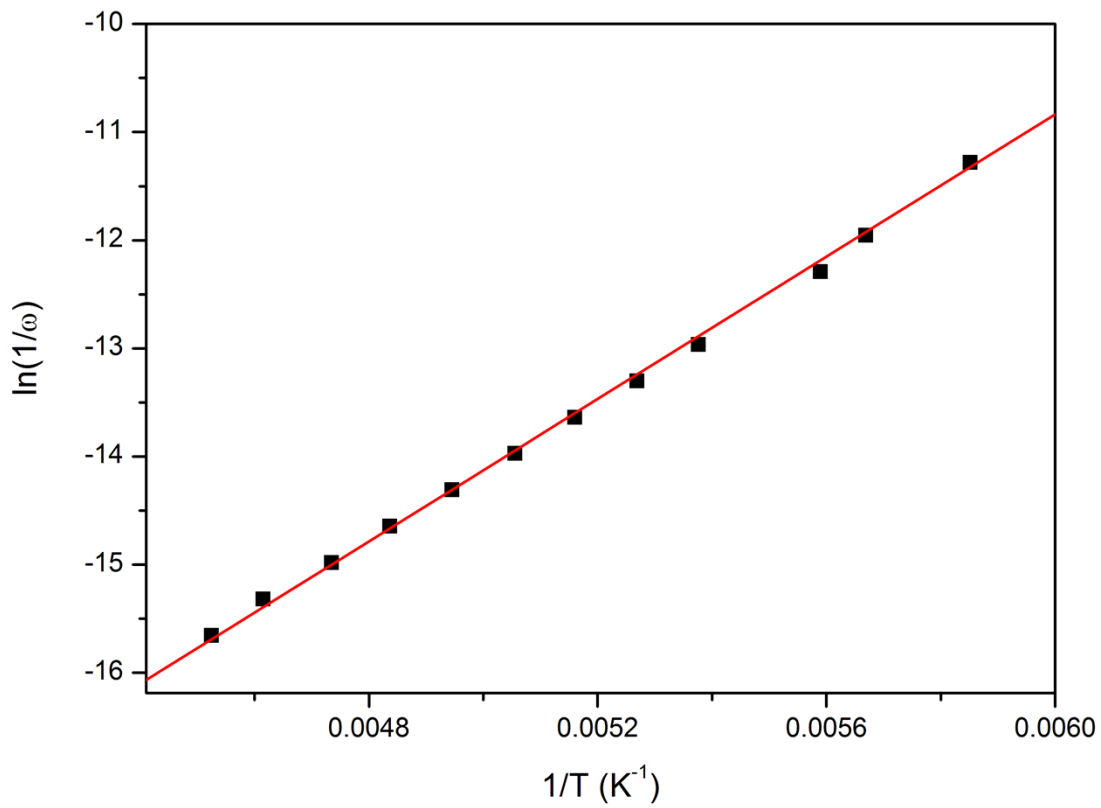


Figure S4. Arrhenius plot of the relaxation frequencies for DMNaFe as a function of inverse temperature. Solid line is the linear fit to the experimental data.

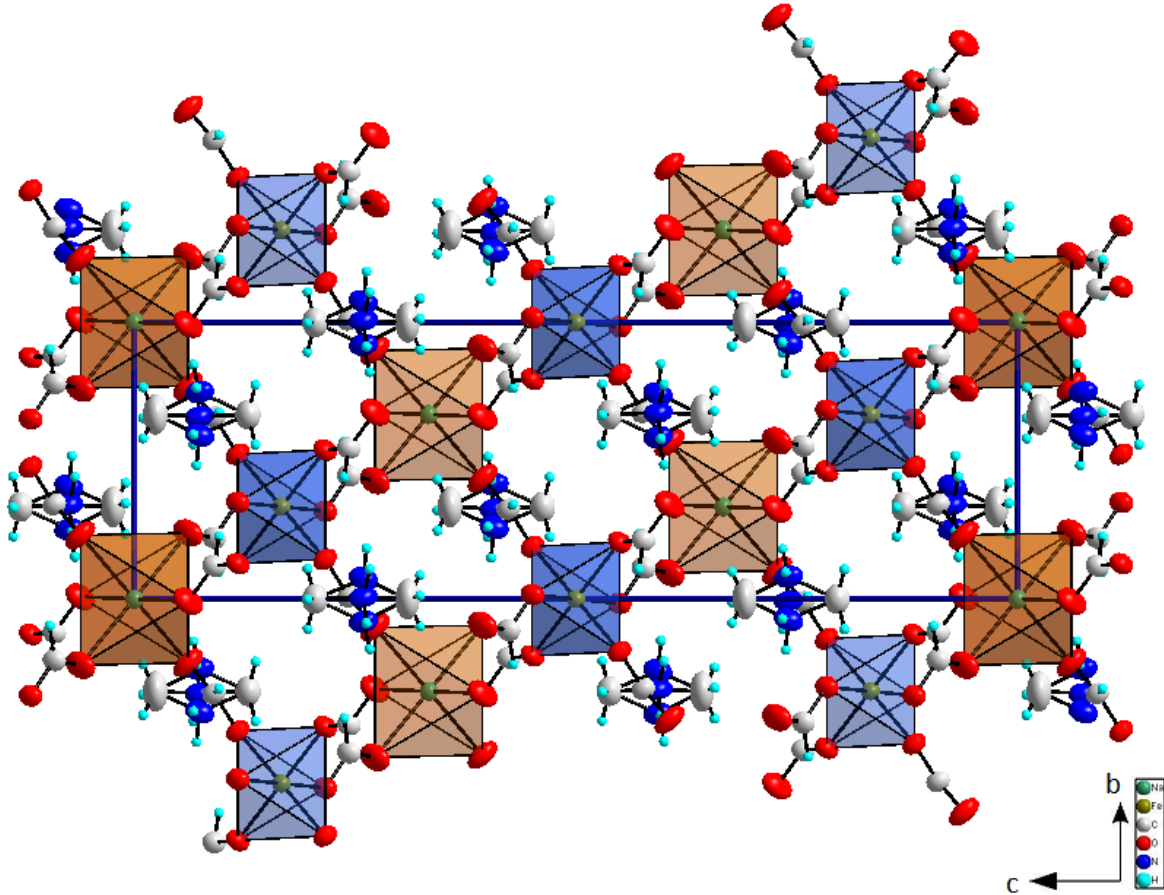


Figure S5. Structure of DMNaFe at 293 K viewed along the *a* axis. Thermal ellipsoids for N atoms of DMA^+ are shown in blue.

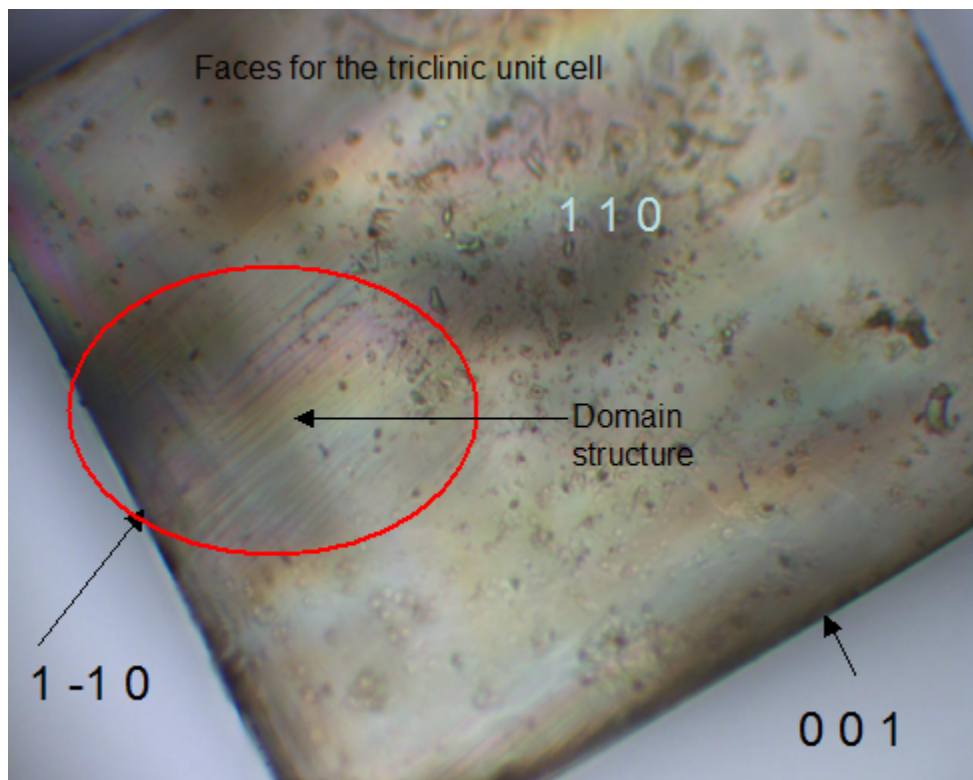


Figure S6. The domain structure of a (110) oriented DMNaFe single crystal observed under a polarizing microscope at 123 K.

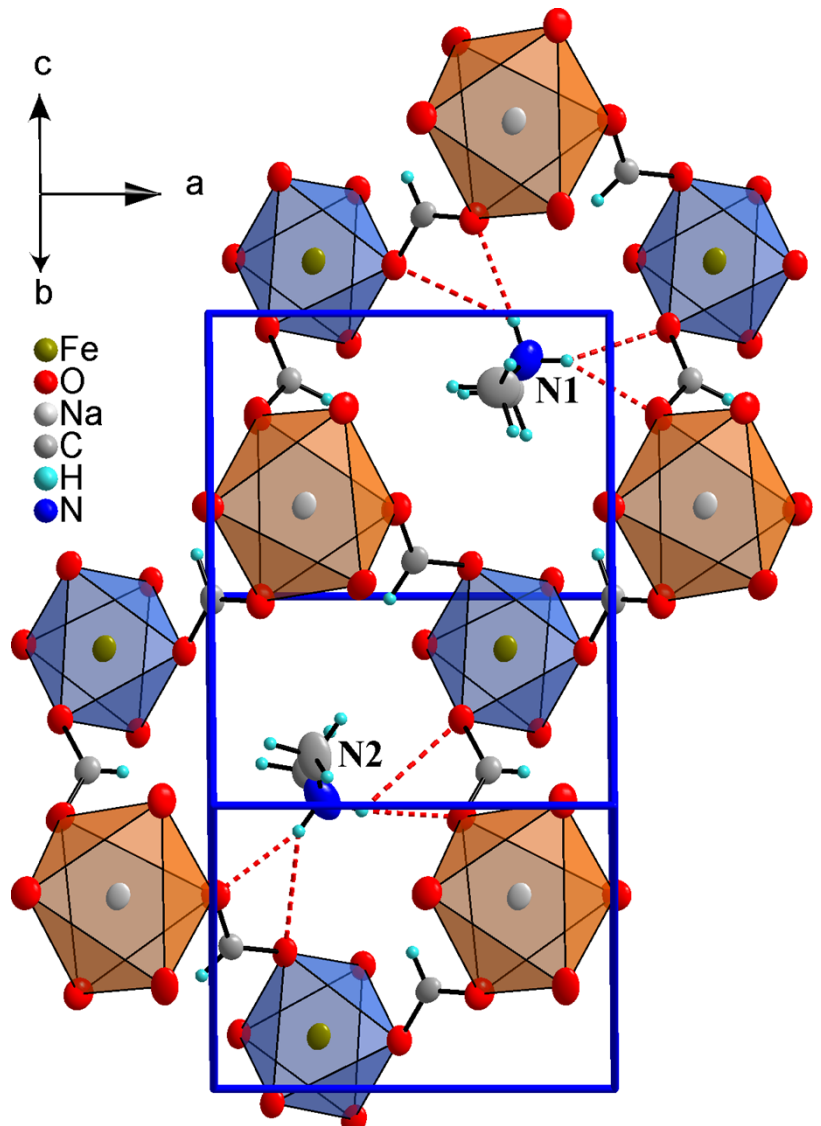


Figure S7. Structure of DMNaFe at 110 K. Thermal ellipsoids for N atoms of DMA⁺ are shown in blue.

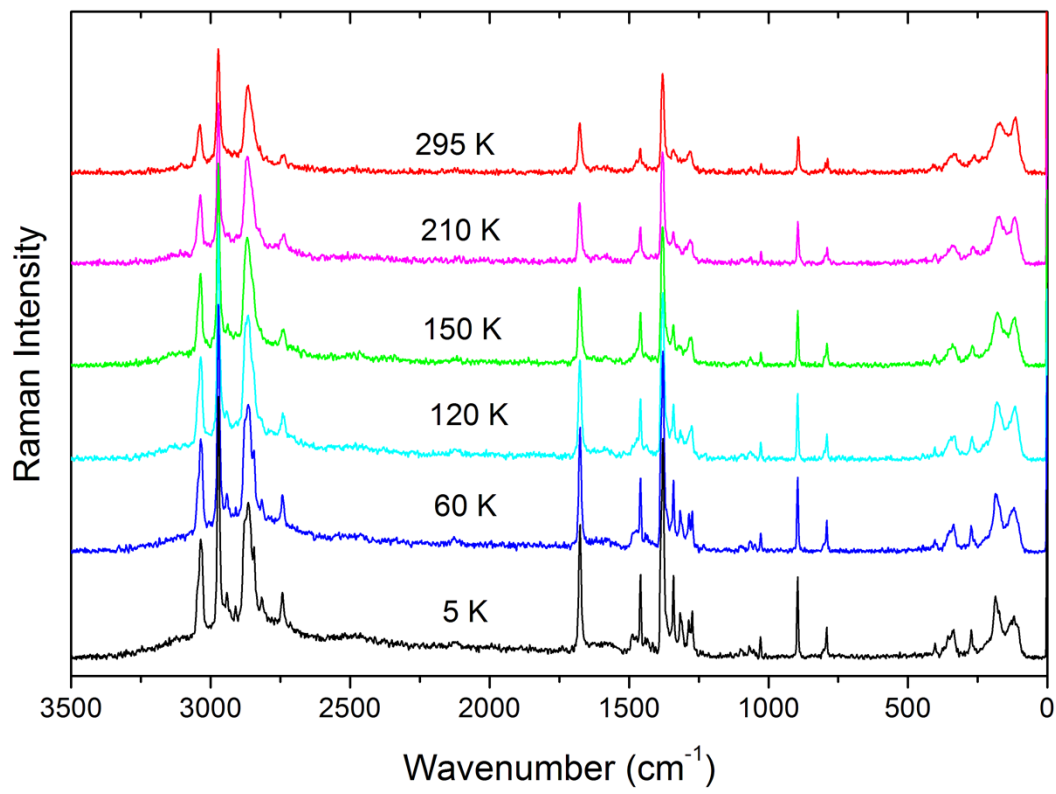


Figure S8. FT-Raman spectra of DMNaFe recorded at various temperatures corresponding to the whole spectral range 80-3500 cm^{-1} .

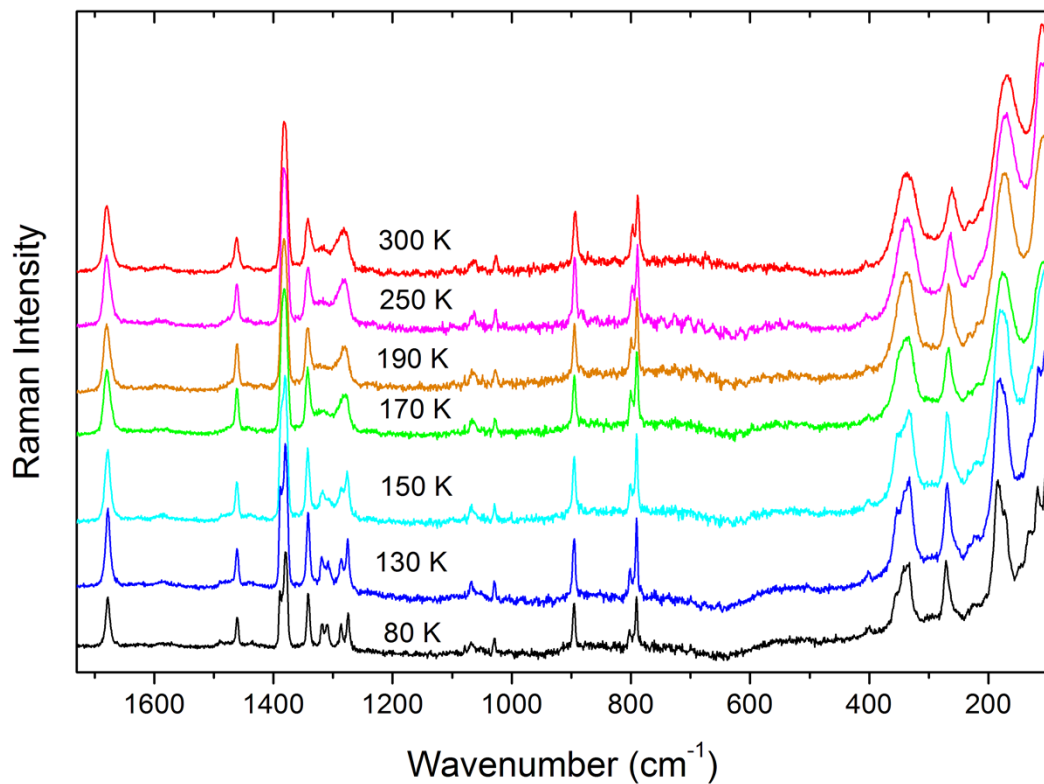


Figure S9. Raman spectra of DMNaFe measured using a Renishaw InVia Raman spectrometer and edge filter at various temperatures corresponding to the spectral range 100-1750 cm⁻¹. The spectra were normalized by the Bose-Einstein factor.

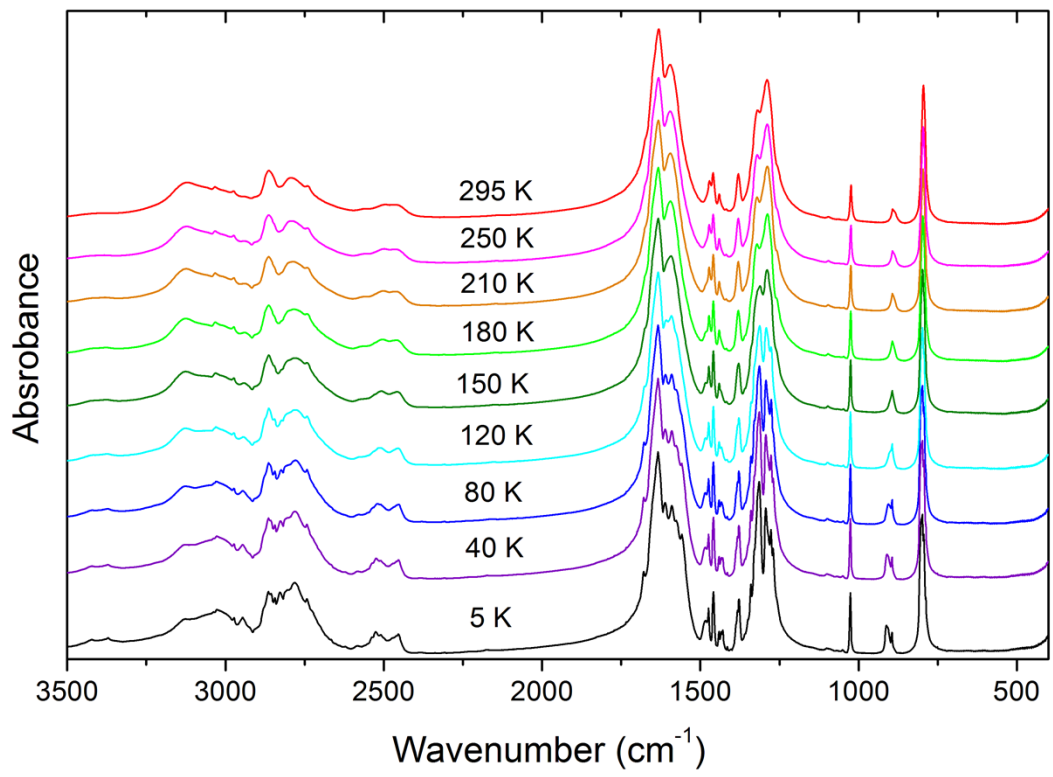


Figure S10. IR spectra of DMNaFe recorded at various temperatures corresponding to the spectral range 400-3500 cm^{-1} .

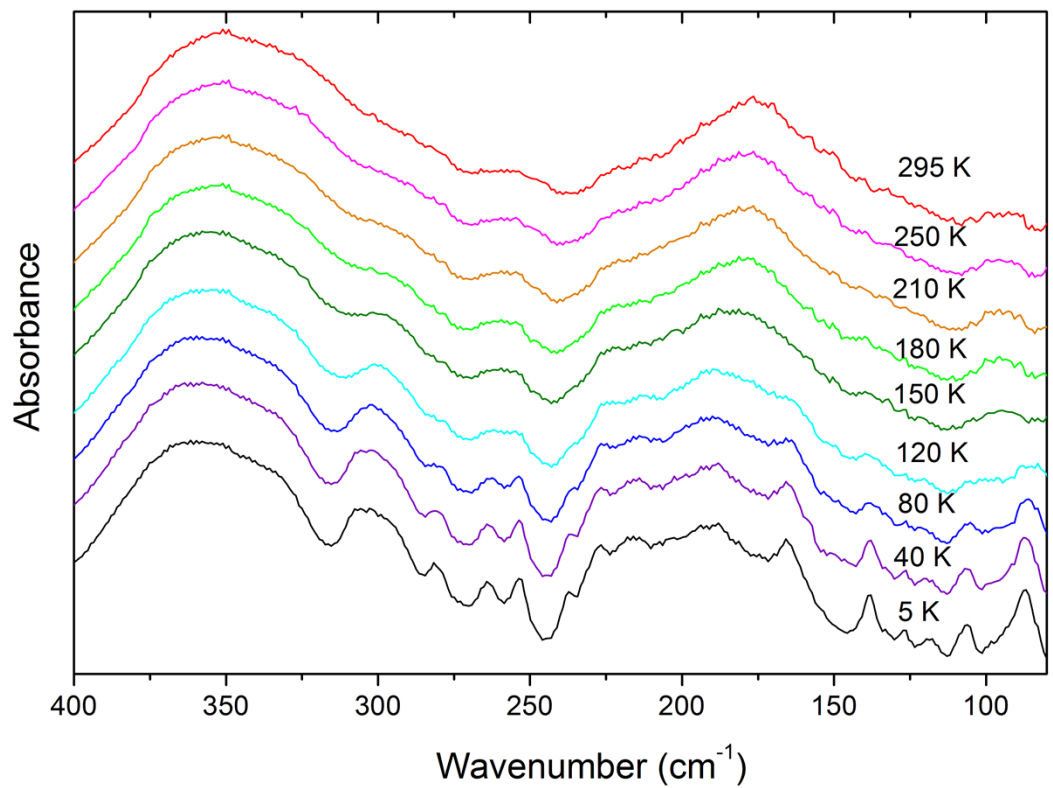


Figure S11. IR spectra of DMNaFe recorded at various temperatures corresponding to the spectral range 80-400 cm^{-1} .

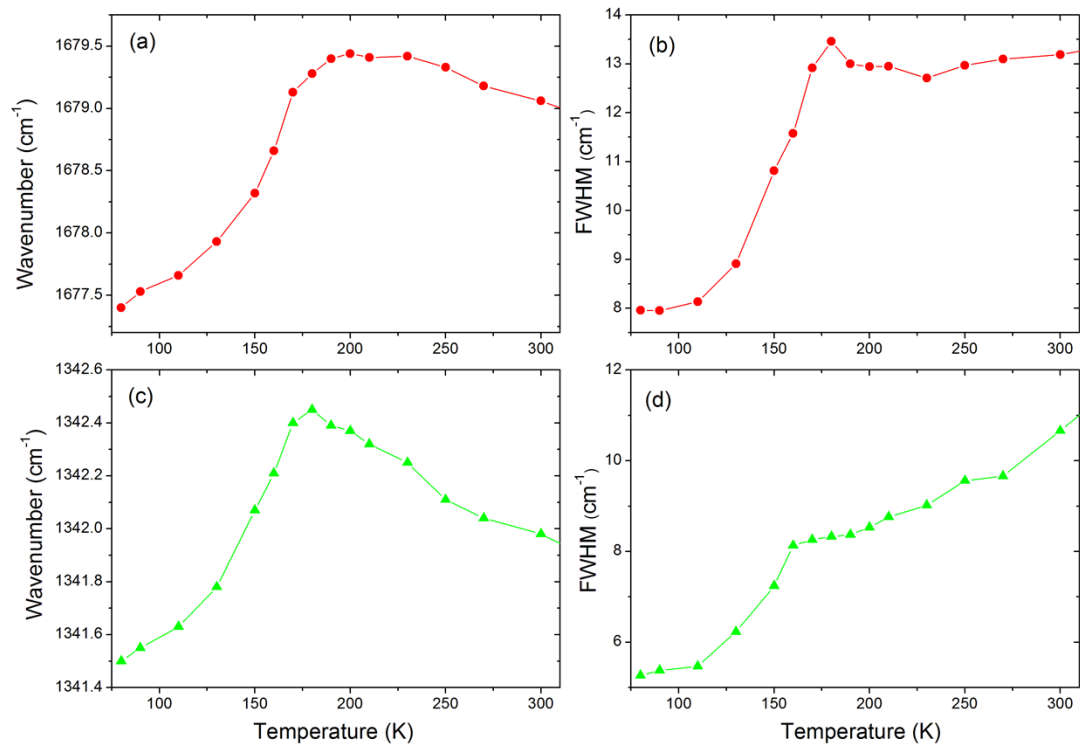


Figure S12. Temperature evolution of (a) 1679 cm^{-1} and (c) 1342 cm^{-1} mode Raman frequencies. (b and d) Temperature evolution of FWHM of the respective modes. Solid lines are to guide the eye.

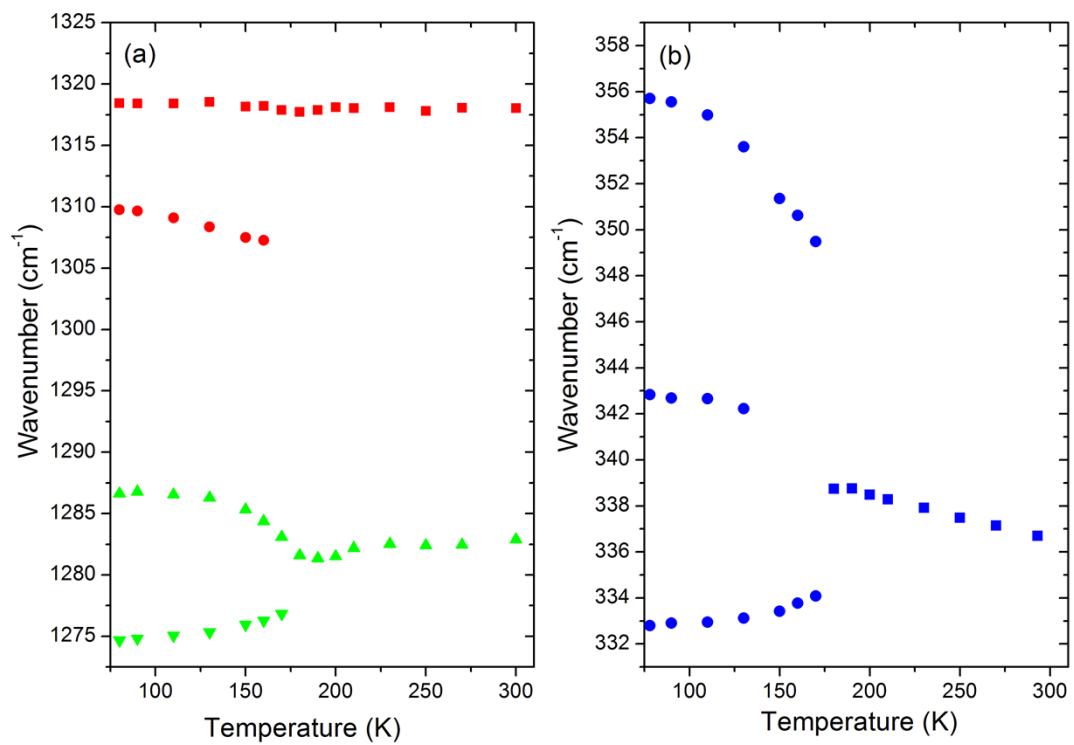


Figure S13. Temperature evolution of (a) $v_2(\text{HCOO}^-)$ and (b) 337 cm⁻¹ lattice mode Raman frequencies.